

Accepted Manuscript

Impact of phenolic resin preparation on its properties and its penetration behavior in Kraft paper

Marion Thébault, Andreas Kandelbauer, Edith Zikulnig-Rusch, Robert Putz, Sandra Jury, Iris Eicher

PII: S0014-3057(18)30500-7

DOI: <https://doi.org/10.1016/j.eurpolymj.2018.05.003>

Reference: EPJ 8401

To appear in: *European Polymer Journal*

Received Date: 14 March 2018

Revised Date: 4 May 2018

Accepted Date: 5 May 2018

Please cite this article as: Thébault, M., Kandelbauer, A., Zikulnig-Rusch, E., Putz, R., Jury, S., Eicher, I., Impact of phenolic resin preparation on its properties and its penetration behavior in Kraft paper, *European Polymer Journal* (2018), doi: <https://doi.org/10.1016/j.eurpolymj.2018.05.003>

This is a PDF file of an unedited manuscript that has been accepted for publication. As a service to our customers we are providing this early version of the manuscript. The manuscript will undergo copyediting, typesetting, and review of the resulting proof before it is published in its final form. Please note that during the production process errors may be discovered which could affect the content, and all legal disclaimers that apply to the journal pertain.



Impact of phenolic resin preparation on its properties and its penetration behavior in Kraft paper

Marion Thébault^a

Andreas Kandelbauer^b

Edith Zikulnig-Rusch^a

Robert Putz^a

Sandra Jury^a

Iris Eicher^a

a: Kompetenzzentrum Holz (Wood K Plus), Altenberger Straße 69, A-4040 Linz;

*c/o: Kompetenzzentrum Holz (Wood K Plus), Wood Carinthian Competence Center (W3C), Klagenfurter
straße 87-89, 9300 Sankt Veit an der Glan, Austria;*

*b: Hochschule Reutlingen, Fakultät Angewandte Chemie, Alteburgstraße 150, D-72762 Reutlingen,
Germany.*

Abstract

The core of decorative laminates is generally made of stacked Kraft paper sheets impregnated with a phenolic resin. As the impregnation process in industry is relatively fast, new methods need to be developed to characterize it for different paper-resin systems. Several phenolic resins were synthesized with the same Phenol: Formaldehyde ratio of 1:1.8 and characterized by Fourier Transform Infrared Spectrometry (FTIR) as well as Size-Exclusion Chromatography (SEC). In addition, their viscosities and surface tensions when diluted in methanol to 45% of solid content were measured. The capacity of each resin to penetrate a Kraft paper sheet was characterized using a new method which measures the conductivities induced by the liquid resin crossing the paper substrate. With this method, crossing times could be measured with a good accuracy. Surprisingly, the results showed that the penetration time of the resin samples is not correlated to the viscosity values, but rather to the surface tension characteristics and the chemical characteristics of paper. Furthermore, some resins had a higher swelling effect on the fibers that delayed the crossing of the liquid through the paper.

Keywords: Phenol; Formaldehyde; Resin; Penetration; Impregnation; Paper.

Introduction

High Pressure Laminates (HPL) are boards of relatively high density, around 1.35 according to standards ISO EN 4386, which are used in different applications of furniture [1,2], electronics [3] and construction [4,5]. During the manufacturing of such decorative laminates, different impregnation process

phases are included. [1,6–8]. In general, HPLs are constituted of a core, impregnated with phenolic (PF) resins, and a decorative surface, impregnated with urea-formaldehyde (UF) and additionally coated with melamine-formaldehyde (MF) or melamine-urea formaldehyde (MUF) resins [1,9,10]. For the core part, Kraft papers with a raw paper weight of 80–260 g/m² and impregnated with a PF resin are compacted together under high temperature and pressure [11]. During the industrial impregnation process, the paper is soaked in resin baths and further passed through drying ovens using different rolls. As this process is relatively fast (ranging from 50 to 250 m/min) [12], it is important that the resin spreads rapidly and homogeneously into the paper sheet. As a consequence, the properties of both, paper and resin, must be carefully harmonized to avoid incomplete impregnation before the pressing step as that could result in inferior final laminates quality [12–14].

PF resins synthesized for the laminates industry are mainly water borne low molecular weight liquid resols with good penetration properties and a suitable molecular weight distribution that may be modified by specific additives [15]. Resols are PF resins prepared under basic catalysis; sodium hydroxide is often used for this purpose, although other bases have been studied as well [16]. Methylene bridges are formed by addition of formaldehyde to the *ortho* or *para* reactive sites of the phenol, and further condensate to give complex branched polymers [5,17,18]. The initial addition reaction can be carried out at temperatures as low as 60°C [18–20], whereas subsequent condensation is efficiently occurring within some hours (depending on the reaction conditions like pH and phenol/formaldehyde ratio) at temperatures around 90°C [18]. The influence of the resin properties like molecular weight distribution, polarity, or viscosity on the impregnation behavior is still not fully understood. Hence, in the present study, different phenolic resins were prepared and their behaviors while penetrating a Kraft paper sheet were compared.

When a porous medium is assumed to comprise of a number of vertical, parallel cylindrical pores that are randomly distributed [21], the continuous flow velocity of a liquid in a cylindrical capillaries model (typical piston displacement of menisci) is calculated according to the Lucas-Washburn equation [12,22,23]:

$$L(t)^2 = \frac{\gamma_L \cdot \cos(\theta) \cdot R}{2\mu} t$$

where t is the time (s) for a liquid of dynamic viscosity μ (Pa.s) and surface tension γ_L (mN/m or J/m²) to penetrate a distance L (m) into the capillaries whose pore radius is R (m), via minescus piston displacement mechanism with a contact angle θ .

This equation is frequently employed in numerous studies on porous media imbibition (including papers) until today, since it provides an important basis to describe paper-fluid relationships and penetration kinetics [24–27]. Resin viscosity and total surface tension can be measured with relatively basic analytical equipment often accessible at impregnation plants. However, several objections were raised against using the Lucas-Washburn approach [28,29] and it is difficult to predict the impregnability of a system “resin-paper” when only referring to this theory, as previously discussed in a review [12].

The value of contact angle measurements of a liquid with a complex porous medium such as paper is often rather limited, since the liquid is usually imbibed by the medium rather rapidly. Besides rapid absorption of the probing drop which impedes the measurement, other effects like irregular surface roughness and varying capillary pressures due to the complex porous structure of the paper web, often cause irreproducible and non-representative values for contact angles. Hence, the practically measured values typically do not reflect the true value of the angle θ required by the Lucas-Washburn equation. Moreover, the complex overlap of cellulose fibers in paper results in a wide variety of pore and throat geometries and sizes that can hardly be subsumed with an average pore radius R , as is done by the Lucas-Washburn approach. Even standard methods such as the Klemm and Gurley tests were shown not to correlate properly with paper penetration by liquids [29,30]. Ridgway et al. assessed that it was necessary to consider network structures including connectivity and pore shape and size distributions in order to correlate porosimetry with permeation properties of different samples [30]. That implies to use specific equipment for raw paper characterization which is typically not available or feasible in an industrial laboratory for quality management and/or R&D. A new method for investigating the paper/resin interaction that directly relates to the industrially relevant penetration behavior could be of great interest.

In the present study, different PF resins were prepared under systematic variation of synthesis conditions (2 levels-3 factorial experimental design) and characterized by Fourier Transform Infra-Red spectroscopy (FTIR), Size Exclusion Chromatography (SEC), viscosity and tensiometry measurements. A new device for characterizing the penetration time of liquid drops with porous substrates [31] was used to compare these resins to each other using the same Kraft paper. This study analyzes and discusses the influence of the resin preparation parameters on the time of penetration measured with this recently invented method.

1 Material and methods

1.1 Resin preparation

Phenol 99% and formaldehyde solution 37% in water were supplied by Carl Roth (Karlsruhe, Germany). Solid phenol was preheated to melt and introduced in a 250ml round-bottom flask. The molar ratio of P:F = 1:1.8 for the prepared PF resol was chosen for it was shown to enhance the polydispersity (ratio of average molecular weights M_w/M_n , see section 2.1) of resols [32], which was supposed to lead to significant differences in physical properties between the resins. Sodium hydroxide (catalyst) in pellets was purchased from Sigma Aldrich (Saint-Louis, Missouri, United States). The pellets were dissolved in distilled water to prepare a 45% solution. Different preparations of PF resins were produced by varying the factors pH (factor A, range of pH 8 to 8.5), pre-heating phase (factor B, either none or a pre-heating period of 1 h at 60°C) and reaction time at 90°C (factor C, range from 2 to 3 hours) according to a 2 level-3 factorial

experimental screening design (Table 1). In this orthogonal design, the effect of each single factor is estimated from comparing the average response value from four experiments at the high level of the respective factor with the average of four experiments at the low level of this factor. Non-significant effects are pooled into determination of the experimental error. Hence, no replicates of single experiments were performed. At the end of each synthesis, the reaction mixture was cooled to room temperature.

Table 1: Conditions of preparation of phenolic resins.

2	Resin	3	pH	4	Time of reaction at 60°C (h)	5	Time of reaction at 90°C (h)
6	1	7	8	8	0	9	2
10	a	11	8.5	12	0	13	2
14	b	15	8	16	1	17	2
18	ab	19	8.5	20	1	21	2
22	c	23	8	24	0	25	3
26	ac	27	8.5	28	0	29	3
30	bc	31	8	32	1	33	3
34	abc	35	8.5	36	1	37	3

The potential influence of pre-heating (B-factor) was investigated because such a step is believed to advance the methylation reaction [33] in phenol-formaldehyde mixtures and thereby influence the kinetics and outcome of the subsequent reaction phase of the actual condensation at 90°C. Thus, pre-heating could influence the final oligomer products at the end of synthesis, for instance in terms of molecular mass distribution.

Water is produced during the synthesis and hence, the final liquids tended to separate into two phases. Some preparations where extreme factor level settings were used (such as runs ac and abc) indeed resulted in resins of very low water tolerance. For this reason, vacuum distillation was carried out after the synthesis. The resins were then dissolved in methanol and kept at a maximum temperature of 4°C until further use.

37.1 Resin characterization

37.1.1 FTIR

Fourier Transform Infrared Spectroscopy was performed with a Bruker TENSOR 27 apparel (Bruker Optics GmbH, Ettlingen, Germany) fitted with a DuraScope SensIR detector. The spectra were recorded as

an average of 32 scans with a double-sided forward-backward acquisition mode, in the spectral range between 4000 and 600 cm^{-1} with a resolution of 2 cm^{-1} .

37.1.2 SEC

Resin samples were dissolved in dimethyl formamide (DMF) to yield 5% w/w solutions. The measurements were carried out with a SEC column Jordi DVB-Glucose 10 000 Å, 5 μm , 300 x 7,8mm, fitted with a pre-column Jordi GBR Mixed Bed 30x7,8mm, on a HPLC Agilent 1100+ device. DMF was used as the eluent at a flow rate of 1.0 mL/min. Polystyrene standards having the following molar masses were used for the calibration: 162, 685, 1470, 4700, 9130, 19600, 34800 and 100000 Da. The samples, each 25 μL at 20°C, were injected in the column which was heated at 40°C. A UV detector at 280 nm of wavelength was used at a temperature of 35°C.

37.1.3 Viscosity

The solid contents of resins were adjusted to 45% by dilution in methanol. Dynamic viscosities of the samples were measured with a Physica MCR101 rheometer from Anton Paar, fitted with a conic spindle CP-50-1/01 of 50mm diameter. The measurements were carried out rotating the spindle from 10 to 100 s^{-1} upon some milliliters of resin sample in a metallic cup at a controlled temperature of 25°C. The Herschel-Bulkley I correlation method was used to determine the evolution of viscosity with the shear rate; it was applied in the form $y=a+b \cdot x^p$.

37.1.4 Surface tension

The total surface tensions of resins diluted in methanol (45% solid content) were measured with a DataPhysics DCAT11EC device. The temperature was between 23 and 26°C. At least two measurements per sample were carried out and the average values were used for further evaluation. The samples were mixed before each measurement. The Wilhelmy Balance method [34] was used to calculate the surface tension with a plate PT11 made of platinum-iridium according to DIN 53914 standard.

Supplementary characterizations of resins are reported in another article [35].

37.2 **Resin penetration measurement into Kraft paper**

A new device designed for characterizing the capacity of a liquid to penetrate a porous substrate [31] was used to study the penetration behavior of prepared resin samples (Figure 1). The three electrodes on both sides of the paper sheet measure two conductivities: one on the side of the paper where a drop of liquid is

deposited (Upper electrodes E1 and E2) and the other between the Upper (E1) and Bottom electrode (E3). Both conductivities are temporally registered with a resolution of 2 ms and 0.02 mA. The device was programmed to stop measurements when the value of conductivity between E1 and E3 exceeds 14mA, where it is considered that a clear short-circuit is established between the top and the bottom surfaces of the substrate.

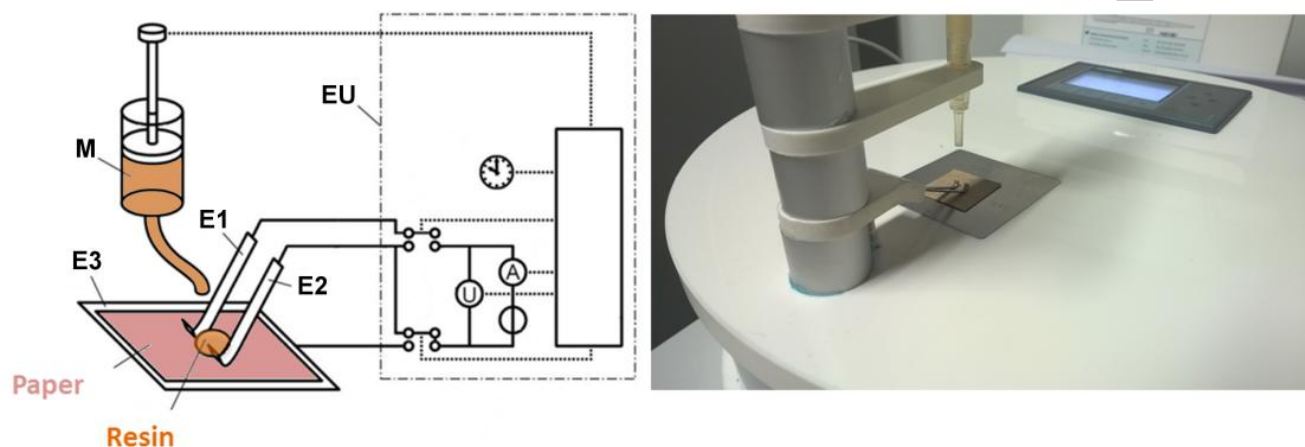


Figure 1: On the left, the scheme of the penetration test device; EU: Electronical Unit system of the device; E1 and E2: Upper electrodes; R: Liquid drop; S: Substrate; E3: bottom electrode; M: Syringe of liquid. On the right, the photography of the device equipped with a resin pipette and a sample of paper sheet.

All resin samples were diluted with methanol to a solid content of 45% and tested with the same paper (Durasorb Saturating Kraft, 250.0 g/m², Caliper 386, Size core 76 mils), supplied from Kapstone Paper and Packaging Corp. (Northbrook, Illinois, United States). The wet strength characteristics were measured 340 ± 20 N/m in cross direction and 566.7 ± 40 N/m in machine direction, and the Gurley air permeation 9 ± 0.6 s. The drops of resins were always put on the top side of the paper sheet. An average value from ten samples was determined for each resin.

The paper pieces and the liquid drops were weighted with a balance with a precision of 1 mg, the tests samples were dried using a hot plate after measurement and weighted one more time to get the specific solid content of each drop.

38 Results

38.1 Resins characteristics

38.1.1 Spectroscopic properties of the prepared resins

The FTIR spectra of the different resin preparation (Figure 2) all presented the same absorbance bands but with different relative intensities depending on the final condition of the preparation. The absorbance bands at 1624 and 1600 cm^{-1} are characteristic for the C=C double bond stretching vibration of aromatic rings and were taken as references to compare the resins. The relative difference of intensity between phenolic and methylol hydroxyl bands at 3700–3000 cm^{-1} and the aliphatic methylene stretch in and out of phase at 2945 and 2885 cm^{-1} , respectively, shows the relative abundance of the methylene bridges formed depending on the reaction conditions. The more the resin preparation protocol favors advancement of condensation, the more distinct the methylene bands become and the signals from unreacted hydroxyl groups are less pronounced. Thus the IR spectra of resins ac, bc and abc differ from the others in having lower intensities of the bands at 3700–3000 cm^{-1} and higher intensities of the bands at 2945 and 2885 cm^{-1} . They also present a smaller shoulder at around 1700–1635 cm^{-1} , which corresponds to the carbonyl functionality (from residual formaldehyde), and more intensive bands of aromatic rings: 3024 cm^{-1} (vibration $\nu(\text{C-H})$), 1510 cm^{-1} ($\nu(\text{C=C})$), 1151 and 1112 cm^{-1} ($d_{\text{ip}}(\text{C-H})$); phenolic: 1365 cm^{-1} ($\nu(\text{C=C})$) and 1224 cm^{-1} ($\nu(\text{C-O})$), and methylene bridges: 1477, 1456 and 1442 cm^{-1} ($d(\text{CH}_2)$) [32,36], which means they are more advanced in condensation than the others.

The absorbance maxima at wavelengths 690, 756, and 823 cm^{-1} represent the number of adjacent hydrogens on the phenolic aromatic ring: five, four and two respectively. The band of three adjacent hydrogen bonds which should appear between 800 and 765 cm^{-1} is only present to a very small extent. The only possible chemical form that correspond to this description is 2,6-dihydroxymethylphenol and its condensed form (where methylene bridges were formed between two phenols instead of two separate phenolic units with unreacted methylol groups).

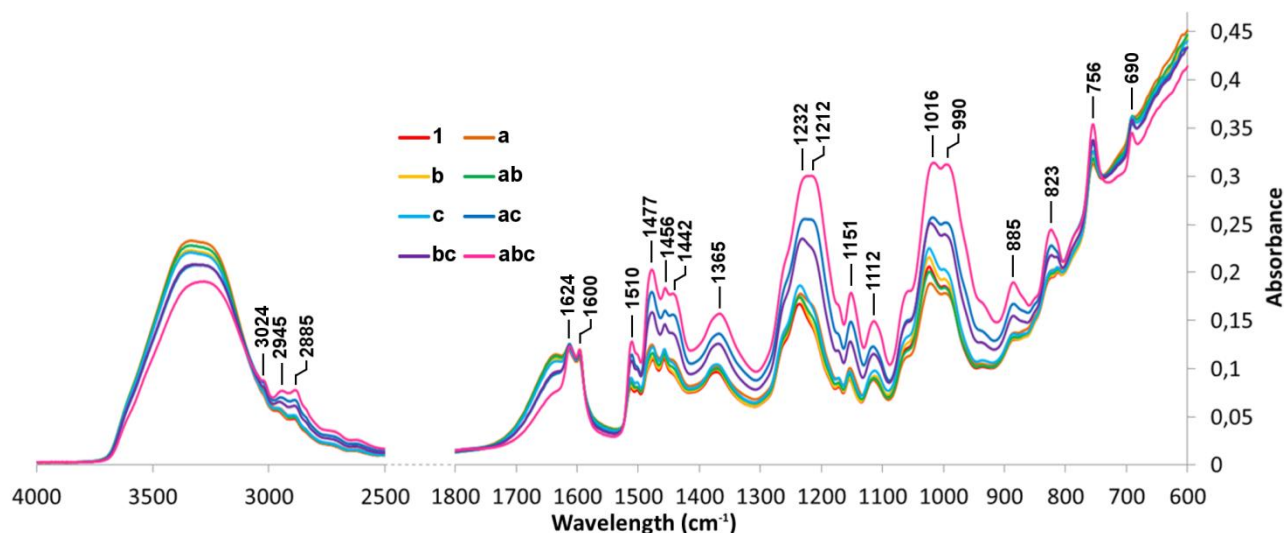


Figure 2: FTIR spectra of the different phenolic resins.

According to Grenier-Loustalot et al. [19], 2,6-dihydroxymethylphenol tends to disappear rapidly because the *para* substituted aromatic carbon is more reactive towards formaldehyde (methylation) or hydroxymethyl groups (condensation) than the *ortho* substituted aromatic carbon. The band at 885 cm^{-1} is characteristic for one hydrogen present in the aromatic ring with different adjacent chemical groups. It is thus typical of phenolic entities with methylol groups or methylene bridges in *para* and *ortho* positions and hence, it should be more intensive for resins at an advanced stage of condensation which is observed with resins ac, bc and abc. The remaining five resins all show approximately the same band intensities, except at 1016 cm^{-1} where the stretching vibration of the methylol group ($-\text{CH}_2\text{-OH}$) occurs: the ratio of relative absorbance of this band on the neighbor one at 990 cm^{-1} (representative of the $-\text{C-H}$ bonds of phenol molecules) is a bit more important in resins prepared at pH 8 (1, b, c and bc) and the resin ab than in the other resins prepared at pH 8.5 (a, ac and abc).

38.1.2 Influence of reaction conditions on average molar mass

The molar mass distribution of each resin measured by SEC is represented in Figure 3 and the calculated number and molar mass averages (M_n and M_w respectively) as well as the polydispersity (M_w/M_n) are listed in Table 2.

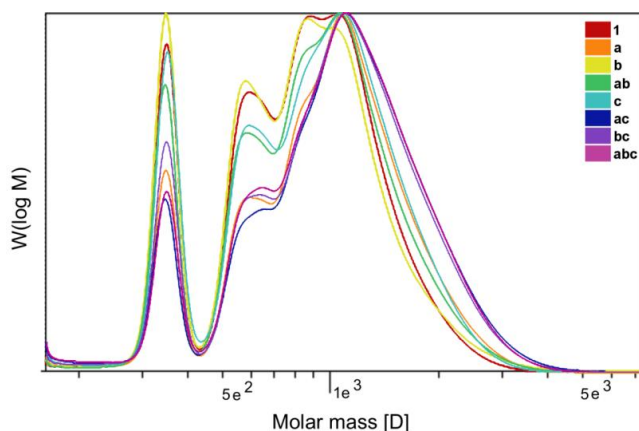


Figure 3: SEC curves of molar mass distribution of the different phenolic resins.

Table 2: Number molar mass average (M_n), mass molar mass average (M_w) and polydispersity index (M_w/M_n) of the different resins.

39	40	41	42
esin	ⁿ (g/mol)	_w (g/mol)	_w / M_n
43	44	45	46
	06	11	.29
47	48	49	50
	98	060	.33
51	52	53	54
	86	160	.69
55	56	57	58
b	40	80	.32
59	60	61	62
	29	80	.34
63	64	65	66
c	53	170	.37
67	68	69	70
c	18	130	.38
71	72	73	74
bc	36	150	.38

The first peak of the molecular weight distribution around 330 g/mol corresponds to oligomers of either 2 phenol units carrying several methylol groups or three phenol units without any methylol groups.

According to Table 2, the values of M_n of the different phenolic resins range from 686 to 853 g/mol, which indicates the presence of oligomers containing 5 to 6 phenol units on average. The general trend of the measurements indicates the increase of molar weight with increasing advancement of the reaction, as expected. This is in accordance with the results from ANOVA analysis of the factorial experiment. For M_n as the response, two significant factors are obtained: the pH (p-value 0.0322) and the reaction time at 90 °C (p-value 0.0261) which both lead to an increase in average molecular weight when changed from low to high level. Application or omission of a pre-heating phase at 60° does not lead to statistically significant changes in molecular weight.

74.1.1 Influence of reaction conditions on viscosity of the PF resins

Viscosity values and surface tension of the resins diluted in methanol are listed in Table 3. Graphs and other supplementary information are available in another article [35]. The usual viscosity range of phenolic resins for paper impregnation purposes is from 15 to 100 mPa.s [37] and generally does not exceed 300 mPa.s for practical reasons [12]. In the present work, the values of viscosity are for most of the resins rather low, which according to the Lucas Washburn equation, would make all of them in principle suitable to rapidly imbibe a porous medium. The variability in resin viscosity depends strongly on the reaction time at 90°C and is generally larger with resins obtained from longer reaction times. The absolute values of viscosity are also larger. More homogenous resins of lower viscosity which behave as Newtonian fluids are obtained with shorter reaction times. Reaction time at 90°C was found to be one statistically significant factor influencing the viscosity to a significant level. This long reaction time always resulted in systematically higher viscosities values.

The combinations of the different factors in the resin preparation lead to different kinds of fluid behaviors that are representative of the polymer chemical interactions. When the reaction time at 90°C is low, the resins are fluid Newtonian liquids, slightly more viscous and dilatant when they are prepared at pH 8.5. When it is high, the pH has a significant influence on the viscosity behavior. On the one hand, resins c and bc have a significant value of viscosity at low shear rates and become less and less viscous as it increases: this is typical of Bingham plastic liquids, which contain particles or large molecules that interact with each other and with the solvent as a one-phase weak solid material. A certain amount of stress is required to break the weak solid structure formed by these particles. As these resins have high molar-weighted molecules with an increased methylation degree compared to resins 1 and b, their capacity to form a pseudo-solid, which cohesion relies on hydrogen bonds, is improved. Once it is broken, the particles move within the liquid under viscous forces. The pre-heating phase at 60°C considerably increases the viscosity values. Since the resin of trial bc exhibits a higher condensation degree than the resin of experiment c (suggested by the analyzes in FTIR and SEC), its higher viscosity was predictable.

On the other hand, the resins ac and abc prepared at pH 8.5 with the longest reaction time at 90°C are becoming more and more viscous with an increasing shear rate: they are dilatant fluids. The dilatant behavior is typical of stabilized suspensions in the liquid phase, e.g. very fine solid particles of polymers dispersed in a solvent. Since these resin polymers are less methylolated than resins b and bc, as suggested by the analyzes in SEC, their interactions via hydrogen bonds between themselves as well as with methanol as solvent are limited; as a result, their dilution in methanol took a longer time to form pseudo-homogeneous phases, because the pre-polymer rearranged in small suspensions. Since the resin ac has higher molar-weighted polymers than the resin abc (Table2), it seems logical that it got bigger suspensions that increase the viscosity in more extent with higher shear rates.

Table 3: Viscosities and surface tensions of the phenolic resins which solid contents were adjusted to 45% by addition of methanol.

Resin number	Viscosity			Viscosity profile	Surface tension (mN/m)
	At 20 s ⁻¹	At 50 s ⁻¹	At 100 s ⁻¹		
1	14.2	14.2	14.3	Newtonian	45.76
a	17.1	18.4	20.4	Newtonian -Dilatant	34.01
b	14.2	14.2	14.3	Newtonian	47.27
ab	15.3	15.6	16.0	Newtonian -Dilatant	40.82
c	49.5	26.8	20.5	Bingham	36.51
ac	27.6	41.9	78.1	Dilatant	29.30
bc	106.0	63.0	52.9	Bingham	33.27
abc	21.5	25.7	32.6	Dilatant	31.13

74.1.2 Influence of reaction conditions on polarity of the PF resins

Concerning the surface tensions, the values of the resins are comprised in a rather large range from 29.30 to 47.27 mN/m. For comparison, the surface tension at 20°C of pure methanol is reported to be 22.45 mN/m and for a highly polar liquid such as water, it is 72.88 mN/m [38]. The surface energy is strongly correlated with the molar mass of the prepared PF resins. Figure 4 displays the correlation between number average molar mass and surface energy. The polarity of the produced polymers is higher for PF resins with a lower average molar mass. This corresponds well with an increased degree of condensation of polar groups at higher degrees of conversion. Both, molar mass and polarity of the resin, are influenced by the pH and the reaction time at 90°C: at the higher levels of these factors, the surface tension is generally lower and the number molar mass average is higher. Accordingly, statistical analysis of the factor effects reveals that only

the factors pH and reaction time at 90 °C have a statistically significant effect (p-values for pH and reaction time are 0.0193 and 0.0056, respectively).

Interestingly, the target responses viscosity and polarity are influenced differently by the reaction conditions: while polarity of the resulting resin is depended on both pH and reaction time at 90°C, the viscosity depends on the factors reaction times at 60°C and 90°C. These results suggest that it should be possible to optimize these two properties independently during chemical synthesis.

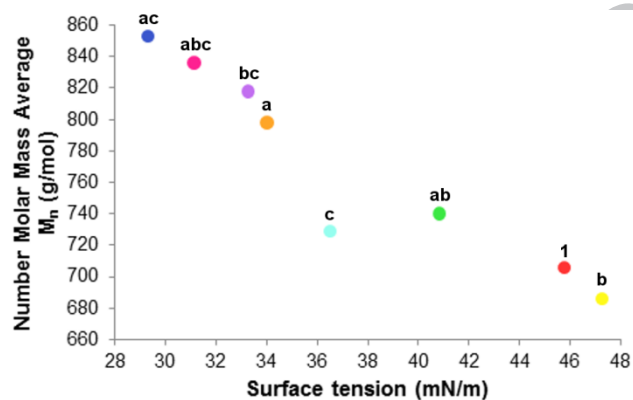


Figure 4: The resins number average molar masses (M_n) versus surface tensions when diluted in methanol (45% of solid content).

74.2 Paper penetration characteristics

A typical characterization with the special device [31] of the crossing of a drop of resin through a sheet of the selected Kraft paper consists in registering two conductivity values, namely the upper (between E1 and E2, see Figure 1), and the bottom electrodes (between E1 and E3). The conductivity measured with the bottom electrode starts to increase after a certain delay and a value of crossing time t_{end} is calculated by measuring the time corresponding to the projected junction of the tangentes as represented in Figure 5. This value is arbitrarily calculated for all the curves according to specific mathematic conditions using the following algorithm: the first tangent is set at the point of maximal first derivative of the conductivity E1-E3, calculated on the central point $\pm 0,4s$. The second tangent is set at a point where the curve of conductivity E1-E3 stabilizes its trend, thus when its second derivative is nearly equal to zero with a threshold of 0,01 mA/s^2 , in average on 4 s. When this condition is found, the point is centred on this interval of 4 s on the curve; otherwise, the average of first derivative on the last 2 s of the measurement is taken and the tangent is set at the end of the curve. The crossing point of both tangents is projected on the conductivity curve between E1 and E3 and the corresponding penetration/crossing time t_{end} is measured.

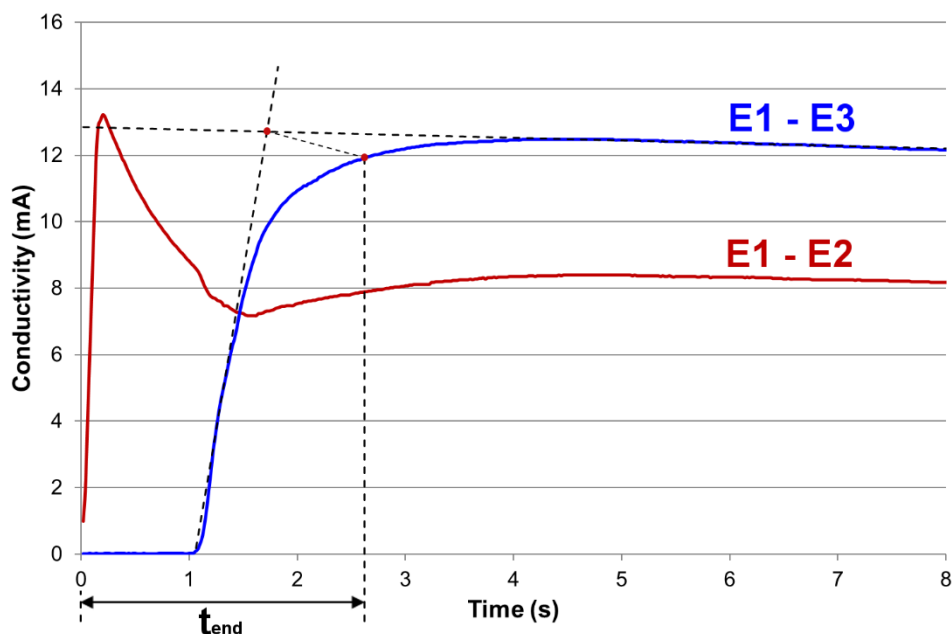


Figure 5: Evolution of conductivity between the upper electrodes (E1 and E2) on the top side of the paper sheet and between the upper and bottom electrodes (E1 and E3) once a drop of resin (c) is set between E1 and E2 (Figure 1). The time of crossing (t_{end}) is here represented.

The conductivity measured between the upper electrodes (E1 and E2) reaches a maximum and starts to decrease after a certain time (0.3 s). This period of decreasing conductivity is mainly due to the spread of the resin drop in the horizontal plane. The liquid may also start to penetrate the paper pores vertically, which contributes to the lower conductivity to some extent. This conductivity then reaches a minimum approximately at t_{end} and slightly increases to stabilize during the next few seconds. This phenomenon might be due to the contact of the liquid with the bottom electrode that could induce a sudden breakage of the fluid flow vertically and an enhancement of the resin spread horizontally, thereby increasing the volume of liquid between the electrodes E1 and E2. Since this effect is not in good and reproducible quantitative correlation with changes in conductivity at the bottom electrode, the value of t_{end} was calculated according to the method described above.

The delay the E1-E3 conductivity takes to rise resembles the wetting delay introduced by Bristow [39] and many others [29]. The wetting delay, highlighted by relative reflectance methods, was measured for instance 0.3 s for a kraft paper with diethylene glycol in Roberts' works [29]. The interpretation of this phenomenon by Bristow was that the liquid takes time to enter large open pores on the surface of paper. It was however contested in other studies [40,41], as the analytical method was not suitable to detect the penetration of micropores by the liquids at the very first microseconds of the contact with the paper. Since kraft is a thick unbleached paper and strongly opaque, the initial wetting on the one side of the paper would not have resulted in any change in reflectance on the surface of the other side of this paper [29].

A similar kind of difficulty to characterize the penetration behaviors at very short time scales occurred during the present study: the measurement of Kraft paper penetration with pure methanol did not give useful results due to the high electrical resistivity ($4.4 \times 10^{-7} \Omega \cdot \text{m}$ versus $4 \times 10^{-8} \Omega \cdot \text{m}$ for water at 18°C [38]) of methanol that impedes the sensor to detect a short circuit. It is possible that the methanol medium of the resin started to penetrate the micropores from the first contact with the paper due to its small molecular size and hence high mobility without being detected by the electrodes.

The plots of all the conductivities measurements for each resin system are shown in Figure 6. Singular curves that look different from the others can be due to the paper local fibers tangle which results in a local lower porosity, that delay the flow of liquid. As the weights of the drops and the specific solid contents of each drops were measured using a precision balance, it appears that these singular curves were performed with drops which presented weights and a specific solid content lower than the average. As these drop are lighter and contain more methanol, they tend to cross the paper sheet more slowly, due to the retention of the methanol by the cellulosic fibers.

For resins prepared at pH 8.5 and a long reaction time at 90°C , the conductivities E1-E2 and E1-E3 have nearly the same trend: a short crossing of the paper thickness represented by the increase of the conductivity E1-E3 (around 0.5 s long) that occurs after a certain delay. In each case, this increase occurs when the conductivity E1-E2 reaches a minimum value, as represented in Figure 5.

For resins 1 and b, conductivities E1-E2 and E1-E3 progress more slowly than for the other resins, although they are very low-viscosity newtonian fluids. However, their surface tensions are very high, 45.76 and 47.27 mN/m respectively, with relatively low molar-weighted molecules (Figure 4). They are therefore more likely to be wicked and retained by the first layer of cellulosic fibers of the paper, which delays the flow through the thickness. Moreover, the conductivities on the top side of the paper (between electrodes E1 and E2) show relatively high levels that do not decrease as fast as for the other paper-resin systems prepared at pH 8.5 (a and ab), that indicates that the liquid tend to stay longer on the top side.

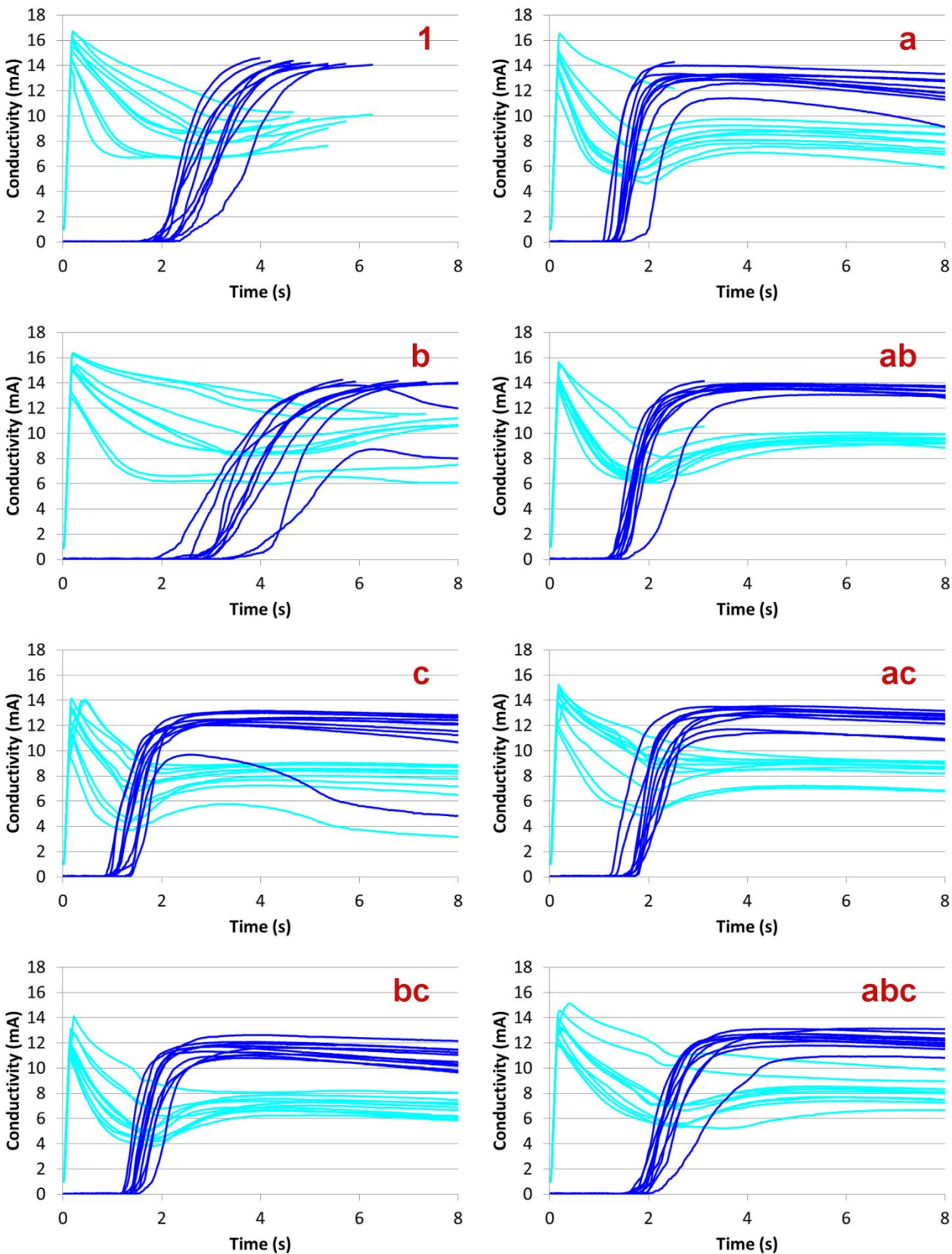


Figure 6: Conductivities curves E1-E2 (light colored) and E1-E3 (dark colored) for each resin.

The results for time of crossing as a measure for the resins ability to penetrate paper are presented in Figure 7, as a scatter plot of penetration time versus resin surface tension. In addition, the values for viscosity at 50 s⁻¹ and the viscosity profiles are given as well in the figure to facilitate interpretation. Resins 1 and b which are the least viscous took the longest to cross the paper sheet, whereas much more viscous resins such as resins ac and bc penetrated the paper sheet more than twice as fast within 2-2.5s. This was rather unexpected since in the literature, the viscosity of a resin is often assumed to be an essential property to judge penetration speed and penetration is generally expected to proceed much faster with more mobile systems, i. e., with resins of low viscosity. Figure 7 instead suggests that polarity in terms of surface tension is much more important, at least for the set of resins with already rather low viscosity studied in the present work. As long as less polar resins are used (below 35 mN/m), penetration times are comparatively low and independent of the viscosity. Resins with similar low polarities but vastly different viscosities ranging from 17.1 to 106.0 at 20 s⁻¹ display practically the same penetration behavior whereas the rather polar systems of low viscosity yielded much longer penetration times. Moreover, Figure 7 suggests that an (although asymmetric) optimum in penetration time is obtained at a surface tension of around 36.5 mN/m. While below this value, reasonably quick imbibition takes place, above this value, penetration speed increases rather quickly. An important conclusion that can be drawn from this work is that short reaction times at 90°C and low pH lead to resins of low viscosities and with many unreacted polar groups, in such a way that they interact strongly with the paper via numerous hydrogen bonds. On the contrary, long reaction times at 90°C and high pH lead to more condensed and unpolar molecules that hardly penetrate the paper pores due to groups of large molecules with little chemical affinity to cellulose. Synthesis of PF resins intended for impregnation should hence be carried out with a strong focus on the fine tuning of their surface energetic behavior. For an overall judgment of course, the cross-linking potential of an impregnation resin must also be considered. If resin c is the fastest to penetrate the paper, it is maybe also because it is constituted of relatively small molecules, which are more mobile than larger ones.

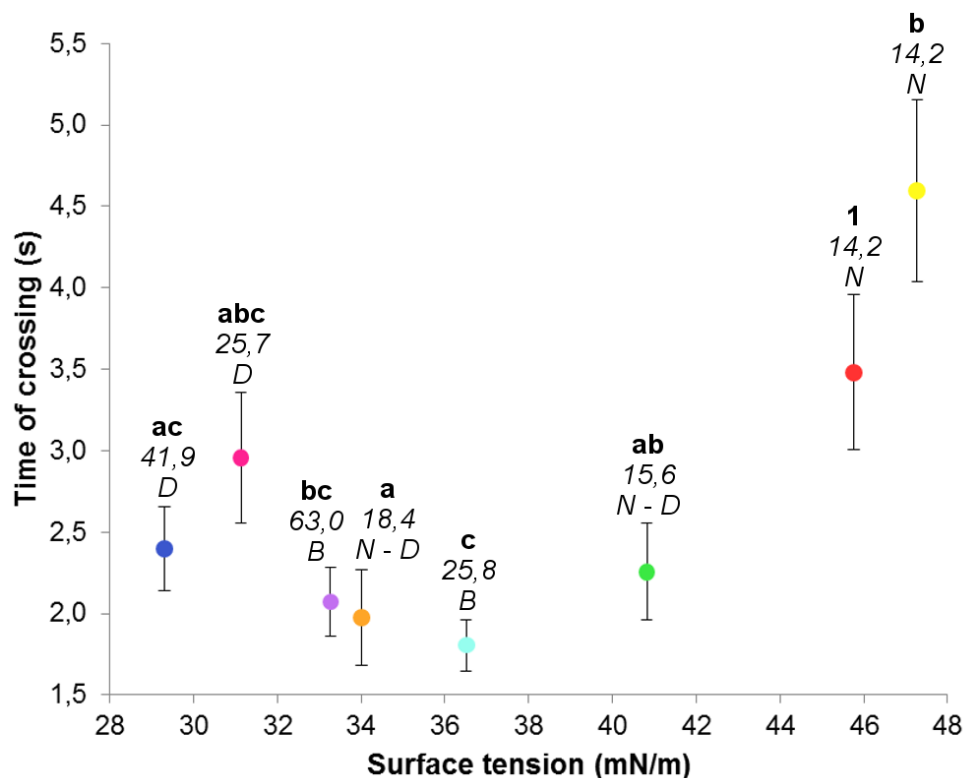


Figure 7: Times of crossing (t_{end}) as function of the surface energy of the different phenolic resins. The corresponding resin numbers (in bold) the viscosity values at 50 s^{-1} in mPa.s, and their viscosity profiles (N: Newtonian; D: dilatant; B: Bingham, in italic) respectively, are shown for each point on the graph.

Regarding the samples of paper where the drop of resin was put (Figure 8), it appears that resin 1 and 3 resulted a lighter color on the paper than the other resins. Furthermore, ripples appeared on the surface as the wetted fibers swelled more strongly than papers impregnated with the other resins. These two resins, 1 and 3, are likely to contain relative small polar molecules, as suggested from the FTIR and SEC analysis. These molecules are likely to enter special clusters of pores such as the micropores of the fibers cell walls, hence a higher swelling effect can be observed than with the other resins. This swelling effect which could be at the origin of the longer time the liquid takes to cross the paper thickness, for the geometric structure of the porous paper is deformed and enlarged during the wicking.

Due to the dark color of the resins, a difference between the top and the bottom surface area of the tested paper sheets is present (Figure 8). This surface area is slightly larger on the bottom side for resins a, ac, bc and abc, which highlights the fact that the penetration is also radial to some extent and not only axial. This effect may be also due to the spread of the liquid on the bottom electrode E3 once the resin reaches E3. Since these resins have less affinity to the paper fibers (which don't retain them) due to their low surface

tensions (below 35 mN/m), they are likely to flow more easily where there are larger voids and air, and have hence a better ability to spread horizontally once they are between the paper and E3.

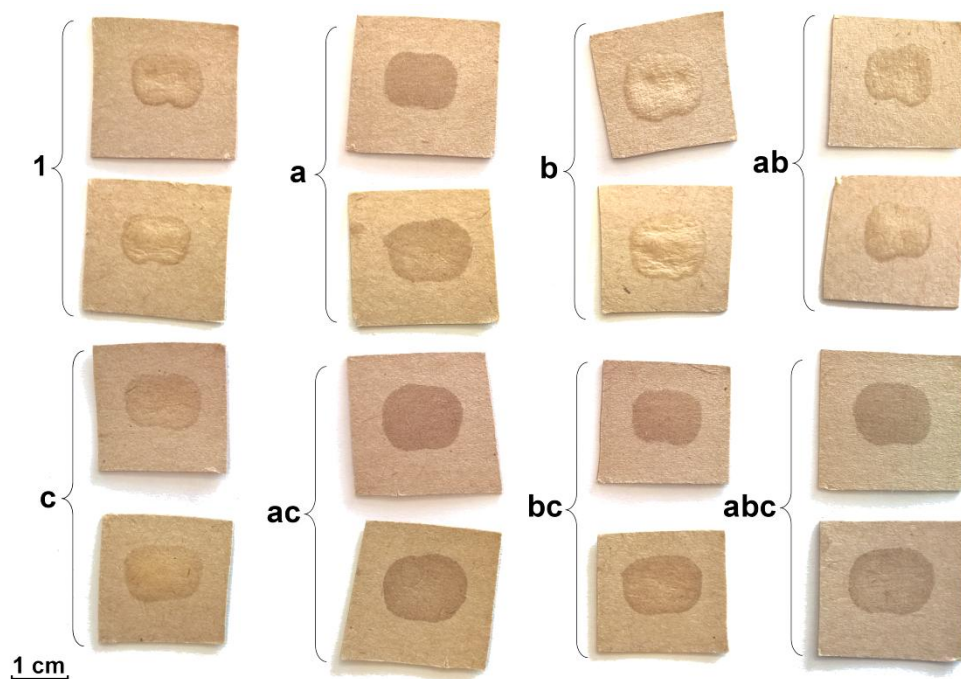


Figure 8: Samples of kraft paper (250g/m²) locally imbibed by a drop of phenolic resin during the measurement of crossing conductivities [31] and then heated to cure the resin. For one test with a resin, the upper image is the top side of the sample where the drop has been put, and the lower image is the view of the same sample on the bottom side.

The values of penetration time between 3 and 5 seconds for a drop of resin do not imply that the paper has not been correctly impregnated. On the other hand, the shortest values of 1.5-2 seconds do not assure a homogenous imbibition of the paper. Nevertheless, when the impregnated paper is strongly swollen, damages in the fibers can appear due to supplementary important deformations caused by the solvent evaporation during the pressing step of the laminate manufacturing. This effect can lead to defects such as voids or delamination and a minor quality of the final board [13].

The lowest values of surface tension as encountered in resins ac and abc (Table 3), 29.30 and 31.13 mN/m in average respectively, do not result in the lowest values of t_{end} , since resins c (pH 8, 0 hour at 60°C, 3 hours at 90°C) and bc (pH 8, 1 hour at 60°C, 3 hours at 90°), respectively 36.51 and 33.27 mN/m in average, cross the paper sheet faster, and resins a (pH 8.5, 0 hour at 60°C, 2 hours at 90°) and ab (pH 8.5, 1 hour at 60°C, 2 hours at 90°), respectively 34.01 and 40.82 mN/m in average, have similar or lower values for this characteristic. Thus, there seem to be an optimal value of surface tension around 36 mN/m where t_{end} is minimal. The total surface tension of a liquid γ_L can be expressed as the sum of intermolecular forces contributions based on the Fowkes theory: non-polar/dispersive γ_L^D and polar γ_L^P , in one of the simplest

forms [12]. These components and their proportions are likely to determine the physico-chemical properties of the liquid resin which can wet the paper fibers easily, i.e that can decrease the value of the contact angle as presented in the Lucas-Washburn equation. Thus it is possible that the values of γ_L^D and γ_L^P for the resin c are the closest to the values γ_s^D and γ_s^P of the paper respectively, making this resin wet the fibers more quickly and cross the sheet in a shorter time than the others.

Conclusion

Phenolic resins with a P:F ratio of 1:1.8 have been synthesized with different pH and cooking time parameters and characterized. Higher pH values and a pre-heating at 60°C generally influence the methylation advancement and the increase of the molar weights polydispersity in the resins. Longer cooking times at 90°C increase the value of the resin viscosity. The resins also showed different values of surface tension which seems to be related to the relative content of methylol groups.

There is a strong interplay between the polarity of the resins (characterized by the surface tension) and the molar mass average. Rather unpolar resins show lower penetration times even if they have a very large molecular weight. Polar resins instead are long in terms of penetration, even if they are of very low molecular-weighted. By increasing the pH and the reaction time at 90°C, one decreases the resin surface tension and increases the M_n value. Hence, it is possible to design resins of rather high pre-condensation degree (rather high molecular weight and correspondingly higher viscosity) while at the same time maintaining preferable penetration behaviour as long as the polarity of the system is kept reasonably unpolar. The present study suggest an upper threshold for the surface tension of the resin of around 38 mN/m for a sufficient penetration time, which may of course be dependent to some extent on the specific type of paper used.

The comparison of the resins regarding their capacity as a drop to be wicked through a saturating Kraft paper with the new method presented here showed, that with the low values of viscosity (lower than 100 mPa.s), the penetration times seem to be rather more influenced by the surface tension values with an optimum around 36 mN/m encountered for the resin made at pH 8, with no pre-heating at 60°C and 3 hours of reaction time at 90°C. The reason which could explain this behavior is the intermolecular interaction between paper (polar surface groups due to cellulose) and resin polar functionalities. A higher surface tension due to a higher content in polar methylol groups seem to make the resin enter the fiber walls of the paper causing a more pronounced swelling which could be the reason of a lower velocity of the fluid front, and, in turn, a higher penetration time.

Thus the presented new method to characterize the liquid penetration of a system resin-paper could be of interest for the laminates industry because of its simplicity and its capacity to provide fast measurements.

Acknowledgments

A part this work was carried out in the COMET program of the Austrian FFG, project number 844608, managed by Kompetenzzentrum Holz GmbH, Sankt Veit, Austria.

The authors thank Dipl. Ing. Jörg Stultschnik for introducing the liquid-substrat penetration device and for the Kraft paper characterization in grammage, mechanical properties and Gurley air permeation. Dipl.-Chem. Dr. Petra Wollboldt is also thanked for having taken part of the phenolic resins analysis in Size Exclusion Chromatography.

References

- [1] K. Lepadat, R. Wagner, J. Lang, Laminates, in: L. Pilato (Ed.), *Phenolic Resins A Century Prog.*, Springer, Berlin, Heidelberg, 2010: pp. 243–261. doi:10.1007/978-3-642-04714-5_11.
- [2] A. Pizzi, K.L. Mittal, *Handbook of Adhesive Technology*, Second Edition, Revised and Expanded, Marcel Dekker, New York, Basel, 2003. doi:10.1080/10426919008953291.
- [3] J.T. Jux, A.M. North, R. Kay, Dielectric properties of standard and modified electrical grade phenol-formaldehyde resin-paper laminates, *Polymer (Guildf)*. 15 (1974) 799–804. doi:10.1016/0032-3861(74)90141-4.
- [4] P.F.Q. de Albuquerque, Phenolic panels for application on exterior facades (in Portuguese), Instituto Superior de Engenharia de Lisboa, 2013. <http://hdl.handle.net/10400.21/3084>.
- [5] F.L. Tobiasson, Phenolic Resin Adhesives, in: *Handb. Adhes.*, Springer US, Boston, MA, 1990: pp. 316–340. doi:10.1007/978-1-4613-0671-9_17.
- [6] L. Burton, A.I. Spear, Decorative laminates, US2857302, 1958.
- [7] J.C. Petropoulos, Multilayer decorative laminate, US3218225A, 1962.
- [8] R.F. Jaisle, T.P. Drees, Decorative laminate, US4473613 A, 1984.
- [9] A. Kandelbauer, G. Wuzella, A. Mahendran, I. Taudes, P. Widsten, Using isoconversional kinetic analysis of liquid melamine-formaldehyde resin curing to predict laminate surface properties, *J. Appl. Polym. Sci.* 113 (2009) 2649–2660. doi:10.1002/app.30294.
- [10] A. Kandelbauer, P. Petek, S. Medved, A. Pizzi, A. Teischinger, On the performance of a melamine-urea-formaldehyde resin for decorative paper coatings, *Eur. J. Wood Wood Prod.* 68 (2010) 63–75. doi:10.1007/s00107-009-0352-y.
- [11] A.B. Figueiredo, D. V. Evtuguin, J. Monteiro, E.F. Cardoso, P.C. Mena, P. Cruz, Structure–Surface Property Relationships of Kraft Papers: Implication on Impregnation with Phenol–Formaldehyde Resin, *Ind. Eng. Chem. Res.* 50 (2011) 2883–2890. doi:10.1021/ie101912h.
- [12] M. Thébault, A. Kandelbauer, U. Müller, E. Zikulnig-Rusch, H. Lammer, Factors influencing the processing and technological properties of laminates based on phenolic resin impregnated papers, *Eur. J. Wood Wood Prod.* 75 (2017) 785–806. doi:10.1007/s00107-017-1205-8.

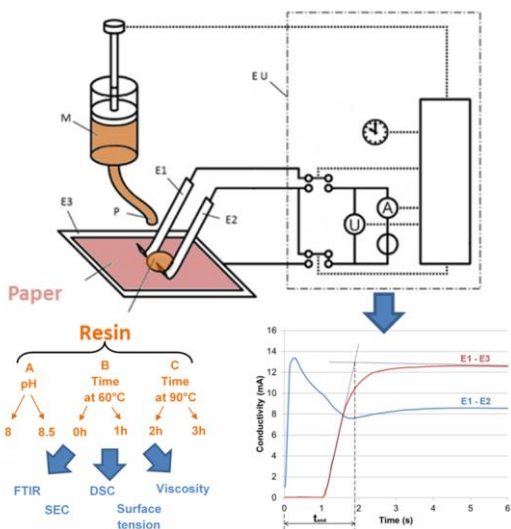
- [13] P. Hubert, A. Poursartip, A Review of Flow and Compaction Modelling Relevant to Thermoset Matrix Laminate Processing, *J. Reinf. Plast. Compos.* 17 (1998) 286–318. doi:10.1177/073168449801700402.
- [14] A. Poursartip, G. Riahi, L. Frederick, X.I.E. Lin, A Method to Determine Resin Flow During Curing of Composite Laminates, *Polym. Compos.* 13 (1992) 58–65. doi:10.1002/pc.750130109.
- [15] European Phenolic Resin Association, Phenolic Resins for Impregnation, (2015). <http://www.epra.eu/21.html> (accessed November 18, 2015).
- [16] M.F. Grenier-Loustalot, S. Larroque, D. Grande, P. Grenier, D. Bedel, Phenolic resins: 2. Influence of catalyst type on reaction mechanisms and kinetics, *Polymer (Guildf)*. 37 (1996) 1363–1369. doi:10.1016/0032-3861(96)81133-5.
- [17] A. Gardziella, L.A. Pilato, A. Knop, Phenolic Resins (2nd Edition), Springer, Berlin, Heidelberg, 2000. doi:10.1007/978-3-662-04101-7.
- [18] L.A. Pilato, Phenolic Resins: A Century of Progress, Springer, Berlin, Heidelberg, 2010. doi:10.1007/978-3-642-04714-5.
- [19] M.F. Grenier-Loustalot, S. Larroque, P. Grenier, J.P. Leca, D. Bedel, Phenolic resins: 1. Mechanisms and kinetics of phenol and of the first polycondensates towards formaldehyde in solution, *Polymer (Guildf)*. 35 (1994) 3046–3054. doi:10.1016/0032-3861(94)90418-9.
- [20] M.F. Grenier-Loustalot, S. Larroque, P. Grenier, D. Bedel, Phenolic resins: 3. Study of the reactivity of the initial monomers towards formaldehyde at constant pH, temperature and catalyst type, *Polymer (Guildf)*. 37 (1996) 939–953. doi:10.1016/0032-3861(96)87276-4.
- [21] C. Ravey, E. Ruiz, F. Trochu, Determination of the optimal impregnation velocity in Resin Transfer Molding by capillary rise experiments and infrared thermography, *Compos. Sci. Technol.* 99 (2014) 96–102. doi:10.1016/j.compscitech.2014.05.019.
- [22] R. Lucas, Rate of capillary ascension of liquids (in German), *Kolloid-Zeitschrift.* 23 (1918) 15–22. doi:10.1007/BF01461107.
- [23] E.W. Washburn, The dynamics of capillary flow, *Phys. Rev.* 17 (1921) 273–283. doi:10.1103/PhysRev.17.273.
- [24] C.J. Nederveen, Absorption of liquid in highly porous nonwovens, *Tappi J.* 77 (1994) 174–180.
- [25] I. Pezron, G. Bourgain, D. Quéré, Imbibition of a Fabric, *J. Colloid Interface Sci.* 173 (1995) 319–327. doi:10.1006/jcis.1995.1331.
- [26] A. Marmur, R.D. Cohen, Characterization of porous media by the kinetics of liquid penetration: the vertical capillaries model, *J. Colloid Interface Sci.* 189 (1997) 299–304. doi:10.1006/jcis.1997.4816.
- [27] G. Callegari, I. Tyomkin, K.G. Kornev, A. V. Neimark, Y. Lo Hsieh, Absorption and transport properties of ultra-fine cellulose webs, *J. Colloid Interface Sci.* 353 (2011) 290–293. doi:10.1016/j.jcis.2010.09.015.

- [28] J. Schoelkopf, Observation and Modelling of Fluid Transport into Porous Paper Coating Structures, University of Plymouth, 2002.
- [29] R.J. Roberts, Liquid penetration into paper, Australian National University (ANU), 2004. <https://digitalcollections.anu.edu.au/handle/1885/49373>.
- [30] C.J. Ridgway, J. Schoelkopf, P.A.C. Gane, A new method for measuring the liquid permeability of coated and uncoated papers and boards, *Nord. Pulp Pap. Res. J.* 18 (2003) 377–381. doi:10.3183/NPPRJ-2003-18-04-p377-381.
- [31] S. Hochsteiner, S. Lenz, J. Stultschnik, Measuring Device and Measuring Method for Measuring the Resin Impregnation of a Substrate, AT517076 (A4), 2016.
- [32] N. Gabilondo, M. Larrañaga, C. Peña, M. a. Corcuera, J.M. Echeverría, I. Mondragon, Polymerization of resole resins with several formaldehyde/phenol molar ratios: Amine catalysts against sodium hydroxide catalysts, *J. Appl. Polym. Sci.* 102 (2006) 2623–2631. doi:10.1002/app.24017.
- [33] J. Monni, L. Alvila, J. Rainio, T.T. Pakkanen, Novel two-stage phenol–formaldehyde resol resin synthesis, *J. Appl. Polym. Sci.* 103 (2007) 371–379. doi:10.1002/app.24615.
- [34] Y. Yuan, T.R. Lee, Contact Angle and Wetting Properties, in: Springer Ser. Surf. Sci. 51, Berlin Heidelberg, 2013: pp. 3–34. doi:10.1007/978-3-642-34243-1_1.
- [35] M. Thébault, A. Kandelbauer, E. Zikulnig-Rusch, I. Eicher, Properties Data of Phenolic Resins Synthetized for the Impregnation of Saturating Kraft Paper, *Data Br.* (2018) [in review].
- [36] I. Poljanšek, M. Krajnc, Characterization of phenol-formaldehyde prepolymer resins by in line FT-IR spectroscopy, *Acta Chim. Slov.* 52 (2005) 238–244.
- [37] W.M. Alvino, H. Mungin, L.G. Brooker, Water-soluble impregnating resins, GB2203746A, 1988.
- [38] J.A. Dean, Lange's Handbook of Chemistry, Fifteenth Edition, McGraw- Hill Inc., 1999. doi:10.1080/10426919008953291.
- [39] J.A. Bristow, Liquid absorption into paper during short time intervals, *Sven. Papperstidning-Nordisk Cellul.* 70 (1967) 623–629.
- [40] D. Eklund, P. Salminen, Water sorption in paper during short times, *APPITA.* 40 (1987) 340–346. <http://cat.inist.fr/?aModele=afficheN&cpsidt=7599956> (accessed January 24, 2017).
- [41] P. Salminen, Studies of water transport in paper during short contact times, Laboratory of Paper Chemistry, Department of Chemical Engineering, Åbo Akademi, 1988.

Highlights

- Eight phenol-formaldehyde resins were synthesized with different parameters.
- The resins were characterized in FTIR, SEC, viscosity and surface tension.
- Resins surface tensions are relatively correlated to the number molar mass average.
- A patented device was used to measure the paper penetration behavior of the resins.
- The penetration is rather correlated to the resin's polarity than to its viscosity.

ACCEPTED MANUSCRIPT



ACCEPTED MANUSCRIPT